HHS Public Access

Author manuscript

Nat Chem Biol. Author manuscript; available in PMC 2016 April 01.

Published in final edited form as:

Nat Chem Biol. 2015 October ; 11(10): 765–771. doi:10.1038/nchembio.1891.

Human Calprotectin Is an Iron-Sequestering Host-Defense Protein

Toshiki G. Nakashige[1], **Bo Zhang**[2], **Carsten Krebs**[2,3], and **Elizabeth M. Nolan**[1,*]

[1]Department of Chemistry, Massachusetts Institute of Technology, Cambridge, MA 02139, USA

[2]Department of Chemistry, Pennsylvania State University, University Park, PA 16802, USA

[3]Department of Biochemistry and Molecular Biology, Pennsylvania State University, University Park, PA 16802, USA

Abstract

Human calprotectin (CP) is a metal-chelating antimicrobial protein of the innate immune response. The current working model states that CP sequesters manganese and zinc from pathogens. We report the discovery that CP chelates iron and deprives bacteria of this essential nutrient. Elemental analysis of CP-treated growth medium establishes that CP reduces the concentrations of manganese, iron, and zinc. Microbial growth studies reveal that iron depletion by CP contributes to the growth inhibition of bacterial pathogens. Biochemical investigations demonstrate that CP coordinates Fe(II) at an unusual hexahistidine motif, and the Mössbauer spectrum of ^{57}Fe(II)-bound CP is consistent with coordination of high-spin Fe(II) at this site (δ = 1.20 mm/s, ΔE_Q = 1.78 mm/s). In the presence of Ca(II), CP turns on its iron-sequestering function and exhibits sub-picomolar affinity for Fe(II). Our findings expand the biological coordination chemistry of iron and support a previously unappreciated role for CP in mammalian iron homeostasis.

Introduction

Transition metal ions are essential nutrients for all organisms.[1] In the vertebrate host, microbial pathogens must acquire first-row transition metal ions including iron, manganese, and zinc, to replicate, colonize, and cause disease.[2–6] Metal-ion withholding is an accepted mechanism of immunity, often termed nutritional immunity,[2,4] and a number of metal-chelating host-defense proteins are utilized during the early stages of infection to prevent microbial acquisition of essential nutrient metals. In humans and other mammals, one of these proteins is calprotectin (CP, S100A8/S100A9 oligomer, MRP-8/14 oligomer,

*Corresponding author: lnolan@mit.edu, Phone: (617) 452-2495, Fax: (617) 324-0505.

Author contributions

T.G.N. and E.M.N. designed the research. T.G.N. prepared the ICP-MS/ICP-OES and Mössbauer spectroscopy samples and conducted the microbial growth assays, ^{55}Fe uptake studies, analytical SEC, ZP1 $K_{d,Fe(II)}$ determination, and metal-ion competition experiments. B.Z. and C.K. performed and analyzed the Mössbauer spectroscopy. T.G.N. and E.M.N. analyzed the results and wrote the paper.

Competing financial interests

The authors declare no competing financial interests.

Supplementary information is available in the online version of the paper.

calgranulins A and B).[4,6–8] Abundant in neutrophils and produced by epithelial cells, CP is released at sites of infection and has antimicrobial activity attributed to its ability to scavenge manganese and zinc.[7–13]

CP is a member of the S100 protein family, and the human form exists as either a heterodimer ($\alpha\beta$) or heterotetramer ($\alpha_2\beta_2$) of S100A8 (α) and S100A9 (β).[14] Each subunit contains two EF-hand domains, at least one of which is understood to bind Ca(II), and two additional sites for transition metal ions form at the S100A8/S100A9 heterodimer interface (Figure 1, Supplementary Results, Supplementary Figure 1).[10–13,15,16] Site 1 is a His_3Asp motif comprised of (A8)His83, (A8)His87, (A9)His20, and (A9)Asp30 (Figure 1b). Site 1 binds Zn(II) with high affinity and has relatively weak affinity for Mn(II).[10,11] Site 2 is an unusual histidine-rich site that was first identified as a His_4 motif comprising (A8)His17, (A8)His27, (A9)His91, and (A9)His95.[16] Subsequent structural[12,15] and spectroscopic[13,15] investigations of manganese-bound CP revealed that site 2 provides a remarkable hexahistidine site for this metal ion with (A9)His103 and (A9)His105 of the S100A9 C-terminal tail completing an octahedral coordination sphere (Figure 1c). Site 2 binds both Mn(II) and Zn(II) with high affinity, and exhibits a thermodynamic preference for Zn(II).[11–13] Moreover, site 2 is important for the antibacterial activity of CP against a variety of Gram-negative and Gram-positive strains.[10,12,13] Loss of site 2 (e.g. ΔHis_4 or AAA mutant, Supplementary Table 1) is reported to be more detrimental to the antimicrobial activity of CP than removal of site 1 (ΔHis_3Asp).[10,12,13] Because site 2 is the high-affinity Mn(II) site, the broad-spectrum antimicrobial activity of CP has been attributed to Mn(II) deprivation.[12] Indeed, a significant body of recent work indicates that various human pathogens (e.g. *Staphylococcus aureus*, *Streptococcus pneumoniae*, *Borrelia burgdorferi*) must acquire manganese to be virulent.[17–20] A robust host-defense mechanism to prevent manganese acquisition is therefore important, and to date CP is the only identified Mn(II)-sequestering protein in humans.[8] Nevertheless, we had difficulty accepting a generalized Mn(II)-centric model for the antimicrobial activity of CP.[13] The specific metal-ion requirements vary amongst organisms, and some of the bacterial strains less susceptible to the site 2 mutants have minimal metabolic requirements for manganese.[10,12,13,21]

We therefore hypothesized that chelation of another as-yet unidentified first-row transition metal ion at site 2 contributes to the growth inhibitory activity of CP. This hypothesis is contrary to prior reports, which concluded that CP does not bind iron or copper.[8,12,14] Nevertheless, the Irving-Williams series,[22] a tenet of coordination chemistry, describes the relative affinities of a given chelator for divalent first-row transition metal ions (Mn < Fe < Co < Ni < Cu > Zn). Although first defined for small-molecule octahedral metal complexes, this series is often employed to rationalize the relative divalent metal-ion affinities of metalloproteins. The relative Mn(II) and Zn(II) affinities of each CP site ($K_{d,Mn} > K_{d,Zn}$) follow this trend,[10,11,23] and we expected the nitrogen-rich metal-chelating motifs to coordinate first-row transition metals that lie between manganese and zinc in the Periodic Table.

To test our hypothesis, we first employed an unbiased approach to evaluate what metal ions CP sequesters in the context of microbial growth assays. On the basis of these initial studies and subsequent investigations, we uncovered a new dimension of the biological coordination

chemistry and growth inhibitory function of CP. Contrary to current understanding, we discovered that CP inhibits the growth of multiple bacterial strains, including human pathogens, by sequestering iron at the unusual histidine-rich Fe(II) site. Our findings afford a new model for the antimicrobial action of CP and indicate a heretofore-unrecognized role for CP in mammalian iron homeostasis. Moreover, biochemical and spectroscopic investigations of CP reveal high-affinity coordination of ferrous iron at a binding site unique amongst known iron-containing proteins, and thereby expand the biological coordination chemistry of Fe(II).

Results

CP depletes Fe from bacterial growth medium

To evaluate the metal sequestration properties of CP, we performed a series of metal-ion depletion experiments (Figure 2, Supplementary Tables 2–10, Supplementary Figures 2 and 3). We treated a standard growth medium employed in antimicrobial activity assays with CP-Ser or a metal-binding site variant and quantified the amounts of residual Mn, Fe, Co, Ni, Cu, and Zn in the medium with and without CP-Ser/variant treatment by inductively coupled plasma-mass spectrometry (ICP-MS) or -optical emission spectroscopy (ICP-OES). CP-Ser is the heterooligomer of S100A8(C42S) and S100A9(C3S) that we routinely employ in metal-binding studies, and this variant exhibits comparable antibacterial activity to native CP.[10] The metal-binding site variants employed throughout this work have one or more metal-chelating residues replaced by Ala (Supplementary Table 1). The CP-Ser ΔHis_3Asp and ΔHis_4 variants are deletion mutants of the His_3Asp and His_4 binding sites, respectively. We define the His_4 site as the four His residues of site 2 that reside at the S100A8/S100A9 interface (Figure 1, Supplementary Table 1). The AAA variant lacks three histidine residues at positions 103–105 of the S100A9 C-terminal tail, and the ΔΔ variant has neither the His_3Asp nor His_4 site. Because we discovered that the Mn(II) and Zn(II) affinities of CP as well as its antimicrobial activity are enhanced in the presence of excess Ca(II),[10,11] we prepared medium samples with or without a 2-mM Ca(II) supplement. We also reported that β-mercaptoethanol (BME) enhances the antimicrobial activity of both native CP and CP-Ser,[10] and therefore evaluated the effect of this reducing agent on metal depletion. The TSB/Tris buffer growth medium used in these studies is routinely employed for evaluating the antimicrobial activity of CP and contains ~150 nM Mn, ~3 μM Fe, and ~5 μM Zn (Supplementary Table 2). The Mn concentration decreased by a factor of 3 (–Ca(II)) or 6 (+Ca(II)) (Figure 2a), and the Zn concentration decreased by a factor of 50 (−Ca(II) or +Ca(II)) (Figure 2b) when the medium was treated with 250 μg/mL CP (±BME). The relative Mn and Zn levels obtained for medium treated with CP mutants were consistent with two central conclusions from prior Mn(II)- and Zn(II)-binding studies: (i) CP binds Zn(II) with high affinity at both sites 1 and 2, and (ii) CP binds Mn(II) with high affinity only at site 2.[10–12]

CP treatment also resulted in depletion of other first-row transition metals in the growth medium (Supplementary Tables 2–10, Supplementary Figure 2), consistent with our reasoning that one or both interfacial sites accommodate such metals. Most strikingly, 250 μg/mL CP caused Fe to decrease by a factor of 3 (−Ca, +BME) or 30 (+Ca, +BME) (Figure

2c). The Ca(II) dependence indicated that CP binds iron more tightly in the presence of Ca(II), in agreement with our prior studies of Mn(II)[11] and Zn(II)[10] sequestration. The 30-fold decrease in Fe (+Ca(II)) reduced its concentration in the growth medium to ca. 80 nM. Moreover, maximum Fe depletion occurred in the presence of excess BME, suggesting a role of the redox environment for this metal. The relative Fe concentrations obtained following treatment of the medium with CP mutants indicated that the His_6 site, and not the His_3Asp site, was essential for Fe depletion. In total, this analysis revealed that CP removes iron from the growth medium and supported a new hypothesis in which Fe deprivation contributes to the antimicrobial activity of CP.

Fe depletion contributes to bacterial growth inhibition

To examine the effect of metal depletion by CP on bacterial growth, we employed CP-treated medium and a panel of Gram-negative and -positive bacterial strains, all of which have a metabolic iron requirement, in growth assays (Figure 3, Supplementary Figures 4 and 5). We supplemented the CP-treated medium with manganese, iron, and/or zinc, in all possible combinations, to achieve the metal concentrations of the untreated medium and monitored bacterial growth over a 20-h period. In all cases, maximum growth recovery occurred only when the metal supplement contained iron. This phenomenon was most striking for the Gram-negative organisms, where Fe supplementation alone was necessary and sufficient to restore full growth, but was also the case for the Gram-positive strains where both Mn and Fe were required to achieve maximum growth recovery.

In a second series of growth studies, we performed antimicrobial activity assays using *Escherichia coli* and *S. aureus* and compared the growth inhibitory activities of CP-Ser, ΔHis_3Asp, ΔHis_4 and proteins pre-incubated with 0.9 equiv of iron supplied as an Fe(II) salt (Figure 4a,b). Iron pre-incubation attenuated the antimicrobial activity of CP to levels comparable to that of ΔHis_4 and completely blocked the activity of ΔHis_3Asp for both species. These experiments further supported the importance of site 2 in the antibacterial activity of CP against these two organisms, and showed that addition of Fe(II) blocks the activity associated with this site.

In a third series of growth studies, we treated *Lactobacillus plantarum* with CP-Ser, ΔHis_3Asp, ΔHis_4 or the AAA mutant (Figure 4c,d, Supplementary Figure 6). Unlike the organisms described previously, *L. plantarum* has no metabolic iron requirement.[24] The Lactobacilli growth medium employed in our experiments is rich in manganese (~100 μM, Supplementary Table 11), and full growth inhibition was observed (+Ca(II), ±BME) with 500 μg/mL (~20 μM) of CP-Ser, ΔHis_4 and AAA. In contrast, the antimicrobial activity was attenuated completely for ΔHis_3Asp. The Lactobacilli growth medium contains ~10 μM zinc, and we attribute the growth inhibitory function of CP against *L. plantarum* to Zn(II) sequestration by the His_3Asp site (Figure 4e, Supplementary Tables 12 and 13). In total, these growth studies revealed that (i) the antimicrobial activity associated with site 2 cannot be attributed only to manganese chelation; (ii) CP sequesters iron, which inhibits the growth of both Gram-negative and -positive organisms; and (iii) the site dependence will be determined by the metal requirements of a given organism as well as the metal-ion availability.

CP blocks bacterial Fe uptake

In a fourth series of growth studies, we examined uptake of the radioactive isotope ^{55}Fe by *E. coli* and *Pseudomonas aeruginosa* in the absence and presence of CP or the ΔΔ variant (Figure 5). This experiment was initiated by transferring bacteria cultured in a minimal medium to an uptake assay medium containing ~3 mM BME, ~2 mM Ca(II), and ~3 μM $FeCl_3$ (1:9 ratio of ^{55}Fe:unlabeled Fe) with or without 500 μg/mL CP-Ser or the ΔΔ variant. These experiments employed a higher inoculum (OD_{600} = 0.2) than employed for antibacterial activity assays (OD_{600} ~ 0.001; Figure 4a, Supplementary Figure 7), and 500 μg/mL CP is insufficient to inhibit bacterial growth at this cell density. Over the course of a 2-h growth period in the uptake medium, the OD_{600} of the cultures increased from ~0.2 to ~0.6 (*E. coli*) or ~0.4 (*P. aeruginosa*) in the absence or presence of CP-Ser or the ΔΔ variant (Figure 5, lower panels). Quantification of ^{55}Fe uptake over time indicated that the presence of 500 μg/mL CP-Ser in the medium reduced bacterial ^{55}Fe uptake relative to the untreated or ΔΔ-treated cultures following a 2-h incubation (Figure 5, upper panels), by 2- to 3-fold. These results establish that supplementation of growth medium with CP-Ser prevents microbial Fe uptake, and this effect requires the metal-binding sites.

CP coordinates Fe(II) at the histidine-rich motif

Iron exists in several biologically accessible oxidation states.[25] We observed that either BME[10] or dithiothreitol (DTT) enhanced the antimicrobial activity of CP against *E. coli* and *S. aureus*, indicating that the effect is not specific to one reducing agent or microorganism (Supplementary Figure 8). Taken together with the knowledge that CP sequesters iron, the BME/DTT effect provides circumstantial evidence that CP prefers to coordinate Fe(II) over Fe(III). To evaluate this notion, we pre-incubated CP-Ser with Fe(II) or Fe(III), performed analytical size-exclusion chromatography (SEC), and analyzed the fractions for CP-Ser and iron (Figure 6a–c). We observed a SEC peak shift with the addition of Fe(II), but not Fe(III), and established that CP retained Fe(II), but not Fe(III), during elution. The residues of the His_6 site, and not the His_3Asp motif, were required for the Fe(II)-induced peak shift (Figure 6d–f, Supplementary Figures 9–11). These observations provided compelling evidence for Fe(II) complexation at the His_6 site and, in prior work, we observed analogous trends for Mn(II).[13]

In addition, we employed Mössbauer spectroscopy to confirm Fe(II) coordination by CP at the His_6 site. The 4.2-K/53-mT Mössbauer spectrum of CP-Ser in the presence of a substoichiometric amount of ^{57}Fe(II) sulfate (Figure 6g, vertical bars) displays a broad quadrupole doublet. The spectrum is significantly different from that of ^{57}Fe(II) sulfate in buffer (Figure 6g, red line), demonstrating that Fe(II) is binding to CP-Ser. Moreover, the Mössbauer spectra of ^{57}Fe(II)-bound CP-Ser and ΔHis_3Asp (Supplementary Figure 12) are essentially indistinguishable, which strongly suggests that Fe(II) is coordinated at the His_6 site. The spectrum can be simulated either as a single quadrupole doublet with an isomer shift (δ) of 1.20 mm/s and a quadrupole splitting parameter (ΔE_Q) of 1.78 mm/s (Figure 6g, blue line) or as two quadrupole doublets [δ_1 = 1.18 mm/s, $\Delta E_{Q,1}$ = 1.68 mm/s (87%) and δ_2 = 1.21 mm/s, $\Delta E_{Q,2}$ = 2.32 mm/s (13%)]. The latter analysis is supported by the 160-K spectrum, in which the resolution of the two components is enhanced (Supplementary Figure 13). The large isomer shift value of 1.20 mm/s allows unambiguous assignment of the ^{57}Fe

species as high-spin Fe(II) and is consistent with octahedral coordination of Fe(II) by the proposed His_6 site (Supplementary Figure 14). Although the magnitude of ΔE_Q is smaller than those typically observed for high-spin Fe(II) complexes,[26] smaller values of ΔE_Q are well-documented for high-spin Fe(II) complexes.[27–29]

CP binds Fe(II) with unprecedented high affinity

To participate in metal sequestration, CP must chelate the metal with high affinity, and its coordination sphere(s) must disfavor dissociation of the metal. Ferrous iron is a labile $3d^6$ metal ion, and the few reported Fe(II) affinities for metalloproteins and transcription factors are typically low (e.g. $K_d \sim 10^{-6} – 10^{-5}$ M).[30] To probe the Fe(II) affinity of CP, we performed Fe(II) competitions with CP and the Ca(II)-insensitive metal-ion sensor ZP1.[31] Titration of ZP1 with Fe(II) under anaerobic conditions resulted in fluorescence quenching (Supplementary Figure 15), as expected from prior investigations.[31] We determined the Fe(II) affinity of ZP1 by using buffers with fixed concentrations of free Fe(II) that spanned the 10^{-7} to 10^{-16} M range (Supplementary Table 14, Supplementary Figure 16, Supplementary Note). These experiments provided $K_{d1,Fe(II)} = 2.2 \pm 0.3$ pM for ZP1 at pH 7.0. Addition of Fe(II) to mixtures of ZP1 and CP-Ser in the absence of Ca(II) afforded the same fluorescence response as a solution of ZP1 alone, which indicated that CP-Ser (αβ) cannot compete with ZP1 for Fe(II) (Figure 7b,c, Supplementary Note). In the presence of excess Ca(II), native CP, CP-Ser, and ΔHis_3Asp outcompeted ZP1 for Fe(II) (Figure 7a,b, Supplementary Figures 17–19, Supplementary Note). Under these same high Ca(II) conditions, negligible competition was observed for the ΔHis_4 and ΔΔ mutants (Figure 7b), and variable degrees of competition for variants harboring mutations in the S100A9 C-terminal tail region occurred (Supplementary Figure 20).

To further examine the role of the S100A9 C-terminal tail region in Fe(II) coordination, we employed the colorimetric iron indicator ferrozine, which is a bidentate ligand that forms a 1:3 Fe(II):ferrozine complex ($K_{d,Fe(II)} = 3.0 \times 10^{-16}$ M),[32] in competition assays with CP-Ser and five C-terminal tail variants (Supplementary Table 1, Supplementary Figure 21, Supplementary Note). These assays were performed in the presence of 50 equiv of Ca(II). The $[Fe(II)ferrozine_3]^{2+}$ complex exhibits an absorbance feature at 562 nm (27,900 M^{-1} cm^{-1}),[33] and addition of 10 μM CP-Ser or H104A to a solution containing 8 μM Fe(II) and 300 μM ferrozine resulted in a time-dependent loss of the optical absorption band for $[Fe(II)ferrozine_3]^{2+}$ over the course of seven days. The absorption feature at 562 nm appeared with subsequent addition of 10 μM Fe(II) (data not shown), which confirmed that the ability of ferrozine to detect Fe(II) was not compromised during the experiment. These results show that both CP-Ser and H104A sequestered Fe(II) from ferrozine. Amino acid substitutions in the S100A9 C-terminal tail region resulted in attenuated competition. The AAA and AHA (comprising H103A and H105A) variants were unable to sequester Fe(II) from ferrozine, and the single variants H103A or H105A afforded an intermediate behavior (Figure 7b). This set of ferrozine competition assays, combined with the ZP1 competitions (Supplementary Figure 20), confirms that H103 and H105 in the S100A9 C-terminal tail region are essential for Fe(II) sequestration.

Other human S100 proteins, including S100A12, S100A7, and S100B, participate in the homeostasis of transition metal ions, and form homodimers that display sites for transition metal binding at the dimer interface.[23,34–36] Because CP is the only S100 family member to exhibit a His_6 site, we reasoned that other S100 proteins are unable to bind Fe(II) with high affinity. Indeed, the ability of CP to outcompete picomolar-affinity ZP1 for Fe(II) was unique amongst five human S100 proteins evaluated (Supplementary Figure 22, Supplementary Note). This result is consistent with our prior study of Mn(II) sequestration where CP was the only S100 protein observed to sequester Mn(II) from ZP1.[13]

Taken together, the ZP1 and ferrozine competition assays (i) confirmed that Ca(II) ions modulate the Fe(II) affinity of CP, (ii) revealed that CP houses a remarkably high-affinity Fe(II) site consistent with its metal-sequestering function, (iii) implicated H103 and H105 of the tail region in Fe(II) complexation, and (iv) established that the Fe(II)-sequestering ability of CP is unique amongst human S100 proteins that form metal-binding sites at dimer interfaces.

Metal selectivity agrees with the Irving-Williams series

CP binds various first-row transition metal ions with high affinity, consistent with its metal-sequestering contribution to the innate immune response.[9–13] Taken together, reports of its Mn(II)- and Zn(II)-binding properties indicate that site 2 coordinates Mn(II) with K_d < 10 nM and Zn(II) with K_d < 240 pM.[9–12,23] In agreement with expectations based on the Irving-Williams series (*vide supra*), CP has a thermodynamic preference for Zn(II) over Co(II) and Mn(II).[10,11] Based on the Irving-Williams series and relative Mn(II)/Zn(II) and Co(II)/Zn(II) affinities of CP, we reasoned that CP will exhibit a thermodynamic preference for Fe(II) over Mn(II) and Zn(II) over Fe(II). A series of metal substitution experiments, performed in the absence and presence of excess Ca(II), support this notion (Figure 7c–e, Supplementary Figure 23).

First, we employed room-temperature electron paramagnetic resonance (EPR) spectroscopy to determine whether addition of 0.9 equiv of Fe(II) to a pre-incubated solution of 25 μM CP-Ser, 0.9 equiv of Mn(II), and 50 equiv of Ca(II) results in metal substitution at site 2. Both Fe(II)- and Mn(II)-CP are EPR silent at room temperature, whereas unbound or “free” Mn(II) in solution displays a six-line pattern centered at g=2. We allowed the Mn(II)-CP (+Ca(II)) samples with and without added Fe(II) to incubate at room temperature for seven days and, at this time point, we observed that addition of Fe(II) to Mn(II)-CP (+Ca(II)) resulted in a more intense free Mn(II) signal relative to the Mn(II)-CP only control (Figure 7c). Quantification of the free Mn(II) signal revealed that the unbound Mn(II) concentration increased ~5-fold to ~14 μM when Fe(II) was added to the sample (Figure 7d). This analysis indicates that Fe(II) substituted ~60% of Mn(II) that was originally bound to site 2, and that both Fe(II)- and Mn(II)-bound CP exist in solution at this time point. To further probe Mn(II)/Fe(II) selectivity, we designed a ferrozine assay to monitor changes in the concentration of unbound Fe(II) following addition of 0.9 equiv of Fe(II) to a pre-incubated solution of ΔHis_3Asp and 0.9 equiv of Mn(II) in the absence and presence of 50 equiv of Ca(II) (Supplementary Figure 23). In agreement with the conclusions from the room-temperature EPR study, this experiment revealed a time-dependent decrease in unbound

Fe(II) and, in the +Ca(II) condition, showed that ~30% of the Mn(II) was displaced following 24 h.

Next, we extended the ferrozine assay to evaluate the consequences of adding 0.9 or 3 equiv of Zn(II) to a pre-incubated solution of 25 μM ΔHis_3Asp and 0.9 equiv of Fe(II). In agreement with our expectations, we observed that incubation of Fe(II)-bound ΔHis_3Asp with Zn(II) resulted in a time-dependent increase in free Fe(II) in solution (Figure 7e). We performed these experiments in the absence or presence of excess Ca(II), which revealed that Zn(II) more rapidly substitutes for Fe(II) in site 2 when Ca(II) is omitted from the buffer. In total, these experiments demonstrate that the metal selectivity of site 2 agrees with the Irving-Williams series.

Furthermore, that ferrozine assays indicate that the kinetics of metal substitution depend on Ca(II), and Ca(II)-bound CP effectively entraps various first-row transition metals at site 2 (Figure 7e, Supplementary Figure 23). Although site 2 has the expected thermodynamic preference for Zn(II), we contend that site 2 will be populated with various metals *in vivo* because it will effectively sequester the metal ion that binds first. We reason that this scenario occurs in the extracellular space where Ca(II) concentrations are high. Thus, kinetics as well as metal-ion availability at a given biological site will contribute to CP speciation in the biological milieu.

Discussion

Previous investigations addressing the role of CP in the metal-withholding component of the host innate immune response have evaluated its ability to scavenge bioavailable manganese and zinc at sites of infection.[7–13,37] In this work, motivated by the hypothesis that CP chelates other first-row transition metal ions, we first employed an unbiased approach to evaluating which metal ions are sequestered by CP in a standard bacterial growth medium. The results from our experiments show that CP depletes iron from growth medium, and that iron deprivation contributes to its antimicrobial activity against both Gram-negative and Gram-positive organisms. Furthermore, our biochemical and spectroscopic investigations demonstrate that CP captures Fe(II) at a biologically unprecedented hexahistidine coordination motif at the S100A8/S100A9 dimer interface.

Our current results contrast two recent reports, which concluded that CP does not chelate iron.[8,12] The first study analyzed the ability of CP to deplete select divalent cations from a growth medium, and a negligible change in iron concentration (reported as percent atoms in solution) was observed whereas the Mn(II) and Zn(II) levels were reduced.[8] In that experiment, the iron oxidation state and CP speciation were ambiguous. The second investigation reported an iron-binding titration monitored by isothermal titration calorimetry (ITC) where CP-Ser was titrated with iron citrate and no enthalpy change was observed.[12] Whether the iron was in the Fe(II) or Fe(III) form in this experiment is unclear, and stoichiometric Ca(II) was employed. The current work indicates that >20 equiv of Ca(II) are required to fully convert CP into its high-Fe(II) affinity form, in agreement with prior observations for the high-affinity Mn(II) complex.[11] Moreover, when considering metal-binding equilibrium, the counterion introduces another variable. Although our current work

indicates that CP will outcompete citrate for Fe(II) (citrate $K_{d,Fe(II)} \sim 10^{-8}$ M),[38] citrate will affect the metal speciation in solution. Importantly, ferrous iron is susceptible to oxidation and strict anaerobic or reducing conditions are needed for maintaining this oxidation state over the course of an experiment. These caveats illustrate the complexity of this system and the multiple experimental considerations that must be taken into account when studying metal-protein interactions, as well as the factors that come into play when working with a redox-active metal like iron.

Our report of iron sequestration by CP may be considered from multiple perspectives. From the standpoint of metal-binding motifs found in Nature, the histidine-rich site of CP is the first example of a biological Fe(II)-His_6 site and thereby expands the biological coordination chemistry of iron-containing proteins. Because Fe(II) is labile and undergoes rapid ligand exchange, the His_6 coordination motif provides a remarkable mechanism for sequestering Fe(II). On the basis of available binding constants, the Fe(II) affinity of CP far exceeds that of characterized proteins that include *E. coli* Fur and superoxide dismutase.[30,39,40] Thus, the molecular basis for how CP overcomes the inherent lability of Fe(II) and achieves such tight binding warrants further exploration. Guided by recent crystallographic and spectroscopic studies of Mn(II) coordination by CP at site 2,[15] we propose that the C-terminal tail region of S100A9 encapsulates Fe(II) in this site and excludes water molecules from the vicinity of the metal center. Moreover, we anticipate that site 2 will chelate Fe(II) in a nearly idealized octahedral geometry with coordination by the Nε atoms of each His residue, as observed for Mn(II).[12,15] Small-molecule Fe(II) hexaimidazole complexes have been structurally characterized,[41,42] and these coordination complexes may provide helpful benchmarks in further studies of Fe(II)-CP.

Our metal depletion studies indicate that CP also chelates Cu and Ni, as expected on the basis of the Irving-Williams series. Thus, a role for CP in the homeostasis of other transition metal ions is worthy of consideration. Given the propensity of CP to chelate multiple metals (e.g. Mn, Fe, Zn) with high affinity, the metallation and speciation of CP in the biological milieu, as well as its consequences for metal homeostasis, will depend on metal-ion availability in any given microenvironment.

From the perspective of the host/microbe interaction, iron is an essential nutrient for almost all microbes, and its sequestration is an established mechanism of innate immunity.[2,3] Host-defense proteins such as lactoferrin and siderocalin interfere with microbial Fe(III) acquisition.[43,44] To the best of our knowledge, a comparable mechanism to prevent microbial Fe(II) uptake is unidentified even though a number of microbes, including human pathogens, express *feoB*, a gene encoding a ferrous iron transporter, when colonizing the host.[45–48] CP is found in a number of physiological locales, and ferrous iron is prevalent under anaerobic conditions.[25] We propose that CP is a heretofore-unrecognized contributor to mammalian iron homeostasis that serves an Fe(II)-sequestering function in reducing and hypoxic microenvironments, and future efforts will address this notion.

Online Methods

Materials and General Methods

All solvents and chemicals were obtained from commercial suppliers and used as received. All aqueous solutions were prepared using Milli-Q water (18.2 MΩ, 0.22-μm filter). Buffers for metal-binding studies were prepared with Ultrol grade HEPES (Calbiochem), TraceSELECT NaCl (Sigma), and aqueous NaOH (Sigma) in either acid-washed volumetric glassware or polypropylene containers, using Teflon-coated spatulas or polypropylene pipettes to transfer chemicals. For large-scale preparation, buffers were routinely treated with 10 g/L Chelex resin (Bio-Rad) for at least one hour, and the Chelex resin was subsequently removed by filtration (0.22 μm). Stock solutions of metal ions were prepared from highest purity available $CaCl_2$, $(NH_4)_2Fe(SO_4)_2{\cdot}6H_2O$, $FeCl_2$, $FeCl_3$, and $ZnCl_2$ (Sigma) in acid-washed volumetric glassware and were transferred to polypropylene containers. Working stock solutions of metal ions for experiments were prepared immediately before use. All experiments with Fe(II) were conducted anaerobically under a N_2 atmosphere in a Vacuum Atmospheres Company glove box unless noted otherwise, and Fe(II) solutions were prepared using the $(NH_4)_2Fe(SO_4)_2$ salt unless noted otherwise. ^{57}Fe metal powder (Isoflex) was dissolved in 2-fold excess of 2-N sulfuric acid, and the concentration of the resulting $^{57}FeSO_4$ solution was determined using the colorimetric ferrozine assay. Radiolabeled $^{55}FeCl_3$ was obtained from PerkinElmer as a solution dissolved in 0.5 M HCl, and experiments employing ^{55}Fe were conducted 180–210 days after the stock date. Ascorbic acid, an atomic absorption spectroscopy iron standard solution (iron(III) nitrate in nitric acid), trichloroacetic acid, ammonium acetate, and ferrozine for the Fe quantification assay were purchased from Sigma. Zinpyr-1 (ZP1) was synthesized from 2',7'-dichlorofluorescein and di(2-picolyl)amine as described,[31] and 2-mM stock solutions of ZP1 were prepared in DMSO, aliquoted, and stored at –20 °C. All bacterial strains were stored as glycerol stocks at –80 °C. Native and mutant proteins (as well as homodimeric S100A7, S100A9(C3S), S100A12, and S100B) were overexpressed and purified as described elsewhere,[10,11,13] and protein stocks were thawed only once immediately prior to use.

Antimicrobial Activity (AMA) Assays

The growth inhibitory activity of CP was tested by following modified literature protocols.[10,13] At least two different protein stocks and media preparations were employed for all assays.

For evaluating the effect of Fe(II) preincubation on the antimicrobial activity of CP against *Escherichia coli* ATCC 25922 and *Staphylococcus aureus* ATCC 25923, bacterial cultures were inoculated into 5 mL TSB with 0.25% dextrose from freezer stocks or single colonies from agar plates, and incubated at 37 °C on a rotating wheel. At t = 16–20 h, the overnight cultures were diluted 1:100 and incubated at 37 °C on a rotating wheel for t = –2.5 h until OD_{600} ~ 0.6 (mid-log phase). The assay medium, a 62:38 (v:v) ratio of 20 mM Tris-HCl, 100 mM NaCl, 5 mM BME, 3 mM $CaCl_2$, pH 7.5 buffer and TSB with dextrose, was prepared using sterile technique. CP samples were buffer exchanged three times into 20 mM Tris-HCl, 100 mM NaCl, pH 7.5 using pre-sterilized 0.5-mL 10K MWCO Amicon spin

concentrators, and 1.1× concentrated protein stocks (1.1 mg/mL to 68.75 μg/mL) were prepared in the medium in the absence and presence of 0.9 eq Fe(II). The Fe(II) stock solution was prepared anaerobically and was exposed to the atmosphere during the assay. The OD_{600} ~ 0.6 bacterial cultures were diluted 1:56, and in a flat-bottom 96-well plate (Corning), each well was filled with 10 μL of bacterial culture and 90 μL of protein solution. Each condition was evaluated in duplicate per trial. The plates were sealed with Parafilm and incubated at 30 °C, 150 rpm. At t = 20 h, the OD_{600} values were measured using a plate reader, and the duplicate measurements were averaged for each trial. The bacterial cultures were agitated by shaking or pipetting to resuspend the cultures to homogeneity prior to the OD_{600} measurement. The mean OD_{600} values and SEM are reported (n = 6).

For evaluating the effect of dithiothreitol (DTT) as the reducing agent in the AMA assays against *E. coli* ATCC 25922 and *S. aureus* ATCC 25923, overnight and 1:100 dilution bacterial cultures were grown as described above. The buffer for the assay medium contained 2.5 mM DTT instead of 5 mM BME. Protein samples were buffer exchanged as above, and 10× concentrated protein stocks (10 mg/mL to 625 μg/mL) were prepared in medium ±BME/DTT ±Ca(II). The OD_{600} ~ 0.6 bacterial cultures were diluted 1:500 into medium ±BME/DTT ±Ca(II), and 10 μL of the 10× protein stock and 90 μL of the 1:500 dilution culture were added to each well in triplicate. The plates were sealed with Parafilm and incubated at 30 °C, 150 rpm, and the OD_{600} was measured at t = 20 h as described above. Three independent trials were conducted, and mean OD_{600} values and standard error are reported (n = 3).

The AMA assays against *Lactobacillus plantarum* WCSF1 were conducted as described above and employed a modified AMA medium. The medium was composed of a 62:38 (v:v) ratio of 20 mM Tris-HCl, 100 mM NaCl, ±5 mM BME, ±3 mM Ca(II), pH 7.5 buffer and MRS medium (CRITERION). The overnight and 1:100 dilution cultures were incubated at 30 °C, 150 rpm.

Metal Analysis

To remove contaminating trace metals, 50-mL Falcon tubes and 15-mL 10K MWCO Amicon spin concentrators were washed with 300 μM EDTA (1×) and Chelex-treated MilliQ water (3×). The materials were then air dried and sterilized by UV-irradiation (t > 15 min) prior to use.

AMA media ±BME ±Ca(II) were prepared using sterile technique. Protein samples were buffer exchanged into 20 mM Tris-HCl, 100 mM NaCl, pH 7.5 using 0.5-mL Amicon spin concentrators, and 2.5 mL of 10× concentrated protein stocks (1.25 or 2.5 mg/mL) were prepared using AMA media ±BME ±Ca(II). The media solutions were prepared in the washed 50-mL Falcon tubes. Untreated (0 μg/mL CP) and CP-treated (125 or 250 μg/mL) media samples were diluted to 25 mL with AMA media ±BME ±Ca(II) and incubated at 30 °C, 150 rpm. At t = 20 h, media samples were filtered in the 15-mL Amicon spin concentrators. The flow through samples were collected and transferred to new, washed 50-mL Falcon tubes. The tubes were sealed with Parafilm, and samples were shipped to and analyzed at the Microanalysis Laboratory at the University of Illinois at Urbana-Champaign. The concentrations of Mn, Co, Ni, Cu, and Zn were quantified by inductively coupled

plasma-mass spectrometry (ICP-MS), and the metal concentrations of Mg, Ca, and Fe were quantified by inductively coupled plasma-optical emission spectroscopy (ICP-OES). At least three independent preparations of media were analyzed for each sample, and analysis of the untreated media +BME ±Ca(II) was conducted during each trial as a control. The mean concentrations (μM and ppm) and the standard error of the mean (SEM) are reported ($n \geq 6$).

Western Blot

To ensure that CP during treatment of growth medium did not pass through the filter, Western blot analysis was employed on CP-treated medium and flow through samples. Sodium dodecyl sulfate-polyacrylamide gel electrophoresis (SDS-PAGE) of the CP-Ser samples was performed on a glycine gel (15% acrylamide). The proteins were transferred to a nitrocellulose membrane following the manufacturer's procedure (BioRad). The S100A8(C42S) and S100A9(C3S) subunits were blotted with polyclonal goat IgG of human calgranulin A (sc-8112) and B (sc-8114), respectively (Santa Cruz Biotechnology). The antibodies were blotted with infrared dye-labeled donkey anti-goat IgG (LI-COR Biosciences), and the blot was visualized using a LI-COR Odyssey Scanner.

Metal-Substitution Bacterial Growth Assays

For the growth assays with *Acinetobacter baumannii* ATCC 17978, *E. coli* ATCC 25922, *E. coli* ATCC 43895 (O157:H7), *Klebsiella pneumoniae* ATCC 13883, *Pseudomonas aeruginosa* PAO1, *Bacillus cereus* ATCC 14579, *S. aureus* ATCC 25923, and *S. aureus* USA300 JE2, bacterial cultures were inoculated from freezer stocks into 5 mL TSB with dextrose and incubated overnight at 30 °C, 150 rpm (*B. cereus*) or 37 °C on a rotating wheel (all other species). At t = 16–20 h, the overnight cultures were diluted 1:100 and incubated at 30 °C, 150 rpm (*B. cereus*) or 37 °C on a rotating wheel (all other species) for t = 2–4.5 h until OD_{600} ~ 0.6 (mid-log phase). AMA media +BME +Ca(II) was treated with 250 μg/mL CP-Ser as described previously for the preparation of the ICP-MS samples, and the OD_{600} ~ 0.6 bacterial cultures were diluted 1:500 into CP-treated or untreated AMA medium. Solutions of 15 μM Mn(II), 300 μM Fe(II), and 500 μM Zn(II) were prepared and filter-sterilized (0.22 μm), and 1 μL of each solution was added to each well of a 96-well plate in all possible combinations. The Fe(II) stock solution was prepared anaerobically and exposed to the atmosphere during dilution into the wells. To each of these wells, 100 μL of bacterial culture was added. The plates were sealed with Parafilm and incubated at 30 °C, 150 rpm, and the OD_{600} was measured every 4 h until t = 20 h. Each condition was conducted in triplicate, and the OD_{600} values were averaged per trial. Three independent trials were conducted, and the mean OD_{600} values and standard error are reported ($n = 3$). To confirm that metal supplementation did not affect the growth of bacteria cultured in untreated medium, this procedure was conducted for the eight bacterial strains with freshly prepared AMA medium with addition of Mn, Fe, Zn, or Mn/Fe/Zn. Two independent trials were conducted, and the mean ± SDM are reported ($n = 2$).

For the growth assays with *L. plantarum* WCFS1, the above procedure was performed with the following modifications. *L. plantarum* cultures were grown at 30 °C, 150 rpm in MRS medium. A modified AMA medium composed of Tris buffer and MRS medium (*vide supra*) was treated with 250 μg/mL CP-Ser. Bacterial cultures diluted 1:500 were supplemented

with 10 μM Mn(II) and/or 10 μM Zn(II) from filter-sterilized 1 mM M(II) stock solutions. The OD_{600} was measured at t = 8 h and 20 h.

^{55}Fe Uptake Assays

Cultures of *E. coli* ATCC 25922 and *P. aeruginosa* PAO1 from single colonies or frozen stocks were grown in M9 minimal medium (1× M9 salts, 2 mM $MgSO_4$, 100 μM $CaCl_2$, 0.25% (w/v) glucose, and 0.2% (w/v) casein) at 37 °C on a rotating wheel for 16–20 h. Overnight cultures were diluted 1:100 into 10 mL of fresh M9 medium and incubated at 37 °C on a rotating wheel until OD_{600} ~ 0.6. Aliquots of cultures (1 mL) were transferred to microcentrifuge tubes and pelleted by centrifugation (3,000 rpm, 7 min, 4 °C). Cells were resuspended with 1 mL of uptake assay (UA) medium (62% (v/v) of 20 mM Tris-HCl, 100 mM NaCl, 5 mM BME, 3 mM $CaCl_2$, pH 7.5; 38% (v/v) M9 medium; supplemented with 2.7 μM $FeCl_3$ and 0.3 μM radiolabeled $^{55}FeCl_3$) with no protein, 500 μg/mL CP-Ser, or 500 μg/mL ΔΔ. The cells were transferred to plastic 15-mL culture tubes, and 3 mL of UA medium with or without protein was added to each tube to afford 4-mL cultures. The cultures were incubated at room temperature without shaking. At t = 30, 60, 90, and 120 min, a 500-μL aliquot of each culture was transferred to a plastic disposable cuvette to measure the OD_{600}. At each time point, 50-μL aliquots of these cultures were transferred to 0.22-μm cellulose acetate centrifuge tube filters (Corning, Inc.). The bacteria were washed with 500 μL of ice-cold wash buffer (50 mM Tris-HCl, 100 mM NaCl, pH 7.5) by centrifugation (3,000 rpm, 1 min, 4 °C) three times to remove extracellular ^{55}Fe. The washed cells were resuspended with a final 500 μL of wash buffer, and the contents of the filter were transferred to liquid scintillation vials containing 9.5 mL of Emulsifier-Safe liquid scintillation fluid. The radioactivity of the cells was measured using a Beckman LS 6500 scintillation counter averaging the counts per minute (CPM) over three minutes. The amount of bacterial ^{55}Fe uptake (reported as nmol of ^{55}Fe per mL of bacteria) was calculated using a calibration curve of CPM vs. standard solutions of $^{55}FeCl_3$ (0–300 pmol). The background radioactivity of the medium and bacteria before supplementation of ^{55}Fe (t = 0) was also measured. The mean ± SEM are reported (n = 4)

Analytical Size-Exclusion Chromatography (SEC)

Analytical SEC experiments were conducted on an ÄKTA purifier with a Superdex 75 10/300 GL column (GE Healthcare Life Sciences) housed at 4 °C. The calibration of the column using a low-molecular-weight calibration kit (GE Healthcare Life Sciences) and SEC elution protocol are described elsewhere.[4] Protein samples (20 μM, 300 μL) were buffer exchanged into 75 mM HEPES, 100 mM NaCl, pH 7.0 buffer prior to experiments. All Fe(II) samples were prepared anaerobically, sealed in microcentrifuge tubes during incubation, and exposed to air immediately before injection onto the SEC column. Protein samples were loaded into a 100-μL loop, and to ensure that the total volume in the loop was transferred to the column, a 500-μL volume was injected. The protein was eluted over 1 column volume of running buffer (75 mM HEPES, 100 mM NaCl, pH 7.0). For samples containing Ca(II), the running buffer contained 2 mM $CaCl_2$.

Ferrozine Fe Quantification Assay

The concentrations of Fe in protein samples were determined following a modified literature protocol.[49] Standards (0 to ~60 μM Fe, 200 μL) were prepared by serial dilution in microcentrifuge tubes using an atomic absorption spectroscopy iron standard solution (iron(III) nitrate in nitric acid). To each sample, 200 μL of 1.5 mM ascorbic acid (dissolved in 0.2 M HCl) and 200 μL of 0.4 M trichloroacetic acid were added, and the resulting solution was heated to 98 °C for 10 min to denature the protein. The solutions were centrifuged to pellet the precipitate (10 min, 13,000 rpm). A 200-μL aliquot of the supernatant was transferred to a new microcentrifuge tube, to which 400 μL of 1.3 M ammonium acetate and 200 μL of 6.17 mM ferrozine were added. The solutions were allowed to incubate for > 5 min at room temperature, and the absorbance at 562 nm was measured.

Protein samples (400 μM, 200 μL) in the absence and presence of 5 equiv of Fe(II) or Fe(III) were prepared. The analytical SEC protocol described previously was performed on these samples, and 0.5-mL fractions were collected in polypropylene tubes. The CP concentration in each fraction was determined by absorbance (ε_{280} = 18,450 M^{-1} cm^{-1}), and 200 μL of the fraction was treated and analyzed as described above. The concentration of Fe in the protein samples was determined employing a standard curve over the concentration range of 0–60 μM Fe.

Optical Absorption and Fluorescence Spectroscopy

Quartz cuvettes with 1-cm path lengths (Starna) were rinsed with 20% nitric acid and thoroughly washed with Milli-Q water prior to use. Protein samples were buffer exchanged into 75 mM HEPES, 100 mM NaCl, pH 7.0 buffer. Optical absorption spectroscopy was performed employing a Beckman Coulter DU 800 spectrophotometer with a Peltier temperature controller. Fluorescence spectroscopy was performed employing a Photon Technologies International QuantaMaster 40 fluorometer outfitted with a continuous xenon source for excitation, autocalibrated QuadraScopic monochromators, a multimode PMT detector, and a circulating water bath. The emission spectra were recorded and integrated using the FelixGX software package. Absorbance and emission spectra were measured at 25 °C.

Mössbauer Spectroscopy

CP samples were buffer exchanged (75 mM HEPES, 100 mM NaCl, pH 7.0) and concentrated to ~2.3 mM. A 370-mM $CaCl_2$ stock solution was prepared and deoxygenated. A 100-mM $^{57}Fe(II)$ stock solution was prepared by dissolving ^{57}Fe metal in 1 M H_2SO_4 and diluting the solution with deoxygenated buffer (75 mM HEPES, 100 mM NaCl, pH 7.0). In microcentrifuge tubes inside the anaerobic glove box, 400-μL solutions of 600 μM CP, 500 μM $^{57}Fe(II)$, and 12 mM Ca(II) were prepared in 90% (v/v) 75 mM HEPES, 100 mM NaCl, pH 7.0 and 10% (v/v) glycerol. After 6 h of incubation under anaerobic conditions at room temperature, 300 μL of the protein solutions were transferred to Mössbauer cups. The samples were placed in an anaerobic cooling chamber chilled with liquid N_2 for 10 min for freezing. The cups housing frozen samples were then quickly stored in insulation vials, and

the filled vials were removed from the glove box and transferred to a storage dewar containing liquid N_2. The samples were stored on dry ice or at −80 °C until analysis.

Mössbauer spectra were recorded on an alternating constant acceleration Mössbauer spectrometer equipped with a Janis SVT-400 variable-temperature cryostat. The external magnetic field at the sample was oriented parallel to the γ-beam. The Mössbauer isomer shifts are referenced relative to the centroid of the spectrum of α-iron at room temperature. Simulations of Mössbauer spectra were carried out using WMOSS spectral analysis software package (www.wmoss.org, SEE Co., Edina, MN).

Mn(II) Substitution Experiment Monitored by EPR Spectroscopy

Continuous-wave room-temperature electron paramagnetic resonance (EPR) spectroscopy was employed to monitor the displacement of Mn(II) from CP by Fe(II). Spectra were obtained using a Bruker EMX spectrometer outfitted with an ER 4199HS cavity and a Bruker Biospin flat quartz cell. Solutions (400 μL) of either 22.5 μM $MnCl_2$ in buffer (75 mM HEPES, 100 mM NaCl, pH 7.0) or 25 μM CP-Ser, 1.25 mM $CaCl_2$, and 22.5 μM $MnCl_2$ with and without the addition of 22.5 μM $(NH_4)_2Fe(SO_4)_2$ were incubated in an anaerobic glove box at room temperature for 7 days. Each sample was removed from the glove box, and immediately transferred to the flat cell. The sample was exposed to air during this time. The room-temperature EPR spectrum was recorded (20-mW microwaves at 9.83 GHz, 1.0-mT modulation amplitude). Using the software SpinCount, the free Mn(II) concentration of each sample was calculated by scaling the inner four lines of the EPR spectrum to that of a 100-μM Mn(II) solution prepared using an atomic absorption standard (Fluka) and measured under identical spectrometer conditions. Three independent trials were conducted, and the mean ± SDM are reported (n = 3).

Fe(II) Substitution Experiment Monitored by Ferrozine

Samples (1.5 mL) of 25 μM CP-Ser ΔHis_3Asp in the absence and presence of 50 equiv of Ca(II) were prepared in 2.0-mL microcentrifuge tubes in the glove box (75 mM HEPES, 100 mM NaCl, pH 7.0). Either Fe(II), Zn(II), or Mn(II) (0.9 equiv) was added, and the mixture was incubated for 30 min. A second metal ion (either 0.9 or 3.0 equiv) was added to the solution. At t = 1, 2, 6, and 24 h after addition of the second metal ion, a 300-μL aliquot of the sample was removed from the glove box and immediately transferred to a 0.5-mL 10K MWCO Amicon spin concentration (Millipore). The sample was centrifuged for 5 min (13,000 rpm, 4 °C). The protein remained in the filter, and 100 μL of the flow through solution containing unbound metal ions was collected. A 100-μL aliquot of the flow through was added to 395 μL of buffer (75 mM HEPES, 100 mM NaCl, pH 7.0) and 5 μL of a 100-mM ferrozine solution (1 mM final concentration). The absorbance at 562 nm was measured after a 5-min incubation. The concentration of unbound Fe(II) was calculated using a standard curve. Additional control samples such as CP-Ser ΔΔ incubated with Fe(II) were also measured following the same protocol. Details of each experimental condition, such as metal concentration and order of metal addition, are described in the text where relevant. Three independent trials were conducted, and the mean ± SDM are reported (n = 3).

Supplementary Material

Refer to Web version on PubMed Central for supplementary material.

Acknowledgements

Research on Fe(II)-CP in the Nolan Laboratory (E.M.N.) was supported by the Office of the Director of the NIH (1DP2OD007045), the MIT Center for Environmental Health Sciences (NIH P30-ES002109), the Sloan Foundation, and the Kinship Foundation (Searle Scholar Award). T.G.N. is a recipient of the NSF Graduate Research Fellowship. Any opinion, findings, and conclusions or recommendations expressed in this material are those of the author(s) and do not necessarily reflect the views of the NSF. We thank Rudiger Laufhutte for performing the ICP-MS and ICP-OES analyses, and Professor JoAnne Stubbe and members of her laboratory for guidance on the ^{55}Fe experiments and for providing the facilities to work with radioactivity. We acknowledge the Network on Antimicrobial Resistance in *Staphylococcus aureus* (NARSA) for providing the *S. aureus* USA300 JE2 strain of the Nebraska Transposon Mutant Library (NTML) supported by NIAID/NIH grant HHSN272200700055C.

References

1. Bertini, I.; Gray, HB.; Stiefel, EI.; Valentine, JS. Biological inorganic chemistry: structure and reactivity. University Science Books; 2007.
2. Weinberg ED. Nutritional immunity: host's attempt to withhold iron from microbial invaders. J. Am. Med. Assoc. 1975; 231:39–41.
3. Fischbach MA, Lin H, Liu DR, Walsh CT. How pathogenic bacteria evade mammalian sabotage in the battle for iron. Nat. Chem. Biol. 2006; 2:132–138. [PubMed: 16485005]
4. Hood MI, Skaar EP. Nutritional immunity: transition metals at the pathogen-host interface. Nat. Rev. Microbiol. 2012; 10:525–537. [PubMed: 22796883]
5. Cassat JE, Skaar EP. Iron in infection and immunity. Cell Host Microbe. 2013; 13:509–519. [PubMed: 23684303]
6. Diaz-Ochoa VE, Jellbauer S, Klaus S, Raffatellu M. Transition metal ions at the crossroads of mucosal immunity and microbial pathogenesis. Front. Cell. Infect. Microbiol. 2014; 4:1–9. [PubMed: 24478989]
7. Sohnle PG, Collins-Lech C, Wiessner JH. The zinc-reversible antimicrobial activity of neutrophil lysates and abscess fluid supernatants. J. Infect. Dis. 1991; 164:137–142. [PubMed: 2056200]
8. Corbin BD, et al. Metal chelation and inhibition of bacterial growth in tissue abscesses. Science. 2008; 319:962–965. [PubMed: 18276893]
9. Kehl-Fie TE, et al. Nutrient metal sequestration by calprotectin inhibits bacterial superoxide defense, enhancing neutrophil killing of *Staphylococcus aureus*. Cell Host Microbe. 2011; 10:158–164. [PubMed: 21843872]
10. Brophy MB, Hayden JA, Nolan EM. Calcium ion gradients modulate the zinc affinity and antibacterial activity of human calprotectin. J. Am. Chem. Soc. 2012; 134:18089–18100. [PubMed: 23082970]
11. Hayden JA, Brophy MB, Cunden LS, Nolan EM. High-affinity manganese coordination by human calprotectin is calcium-dependent and requires the histidine-rich site formed at the dimer interface. J. Am. Chem. Soc. 2013; 135:775–787. [PubMed: 23276281]
12. Damo SM, et al. Molecular basis for manganese sequestration by calprotectin and roles in the innate immune response to invading bacterial pathogens. Proc. Natl. Acad. Sci. U.S.A. 2013; 110:3841–3846. [PubMed: 23431180]
13. Brophy MB, Nakashige TG, Gaillard A, Nolan EM. Contributions of the S100A9 C-terminal tail to high-affinity Mn(II) chelation by the host-defense protein human calprotectin. J. Am. Chem. Soc. 2013; 135:17804–17817. [PubMed: 24245608]
14. Vogl T, Leukert N, Barczyk K, Strupat K, Roth J. Biophysical characterization of S100A8 and S100A9 in the absence and presence of bivalent cations. Biochim. Biophys. Acta. 2006; 1763:1298–1306. [PubMed: 17050004]

15. Gagnon DM, et al. Manganese binding properties of human calprotectin under conditions of high and low calcium: X-ray crystallographic and advanced electron paramagnetic resonance spectroscopic analysis. J. Am. Chem. Soc. 2015; 137:3004–3016. [PubMed: 25597447]
16. Korndörfer IP, Brueckner F, Skerra A. The crystal structure of the human $(S100A8/S100A9)_2$ heterotetramer, calprotectin, illustrates how conformational changes of interacting α-helices can determine specific association of two EF-hand proteins. J. Mol. Biol. 2007; 370:887–898. [PubMed: 17553524]
17. Zaharik ML, Finlay BB. Mn^{2+} and bacterial pathogenesis. Front. Biosci. 2004; 9:1035–1042. [PubMed: 14977526]
18. Papp-Wallace KM, Maguire ME. Manganese transport and the role of manganese in virulence. Annu. Rev. Microbiol. 2006; 60:187–209. [PubMed: 16704341]
19. Jacobsen FE, Kazmierczak KM, Lisher JP, Winkler ME, Giedroc DP. Interplay between manganese and zinc homeostasis in the human pathogen *Streptococcus pneumoniae*. Metallomics. 2011; 3:38–41. [PubMed: 21275153]
20. Aguirre JD, et al. A manganese-rich environment supports superoxide dismutase activity in a Lyme disease pathogen *Borrelia burgdorferi*. J. Biol. Chem. 2013; 288:8468–8478. [PubMed: 23376276]
21. Lisher JP, Giedroc DP. Manganese acquisition and homeostasis at the host-pathogen interface. Front. Cell. Infect. Microbiol. 2013; 3:1–15. [PubMed: 23355975]
22. Irving H, Williams RJP. The stability of transition-metal complexes. J. Chem. Soc. 1953:3192–3210.
23. Brophy MB, Nolan EM. Manganese and microbial pathogenesis: sequestration by the mammalian immune system and utilization by microorganisms. ACS Chem. Biol. 2015; 10:641–651. [PubMed: 25594606]
24. Archibald FS, Fridovich I. Manganese and defenses against oxygen toxicity in manganese and defenses against oxygen toxicity in *Lactobacillus plantarum*. J. Bacteriol. 1981; 145:442–451. [PubMed: 6257639]
25. Frey PA, Reed GH. The ubiquity of iron. ACS Chem. Biol. 2012; 7:1477–1481. [PubMed: 22845493]
26. Münck, E. Physical methods in bioinorganic chemistry: spectroscopy and magnetism. Que, L., Jr, editor. University Science Books; 2000. p. 287-319.
27. Greenwood, NN.; Gibb, TC. Mössbauer spectroscopy. Springer; 1971.
28. Asch L, Adloff JP, Friedt JM, Danon J. Motional effects in the Mössbauer spectra of iron(II) hexammines. Chem. Phys. Lett. 1970; 5:105–108.
29. Bossek U, et al. Exchange coupling in an isostructural series of face-sharing bioctahedral complexes $[LMII(\mu\text{-}X)_3M(II)L]BPh_4$ (M = Mn, Fe, Co, Ni, Zn; X = Cl, Br; L=1,4,7-trimethyl-1,4,7-triazacyclononane). Inorg. Chem. 1997; 36:2834–2843. [PubMed: 11669919]
30. Cotruvo JA Jr, Stubbe J. Metallation and mismetallation of iron and manganese proteins *in vitro* and *in vivo*: the class I ribonucleotide reductases as a case study. Metallomics. 2012; 4:1020–1036. [PubMed: 22991063]
31. Walkup GK, Burdette SC, Lippard SJ, Tsien RY. A new cell-permeable fluorescent probe for Zn^{2+} J. Am. Chem. Soc. 2000; 122:5644–5645.
32. Gibbs CR. Characterization and application of ferrozine iron reagent as a ferrous iron indicator. Anal. Chem. 1976; 48:1197–1201.
33. Stookey LL. Ferrozine—a new spectrophotometric reagent for iron. Anal. Chem. 1970; 42:779–781.
34. Moroz OV, Blagova EV, Wilkinson AJ, Wilson KS, Bronstein IB. The crystal structures of human S100A12 in apo form and in complex with zinc: new insights into S100A12 oligomerization. J. Mol. Biol. 2009; 391:536–551. [PubMed: 19501594]
35. Brodersen DE, Nyborg J, Kjeldgaard M. Zinc-binding site of an S100 protein revealed. Two crystal structures of Ca^{2+}-bound human psoriasin (S100A7) in the Zn^{2+}-loaded and Zn^{2+}-free states. Biochemistry. 1999; 38:1695–1704. [PubMed: 10026247]

36. Ostendorp T, Diez J, Heizmann CW, Fritz G. The crystal structures of human S100B in the zinc- and calcium-loaded state at three pH values reveal zinc ligand swapping. Biochim. Biophys. Acta. 2011; 1813:1083–1091. [PubMed: 20950652]

37. Liu JZ, et al. Zinc sequestration by the neutrophil protein calprotectin enhances *Salmonella* growth in the inflamed gut. Cell Host Microbe. 2012; 11:227–239. [PubMed: 22423963]

38. Königsberger LC, Königsberger E, May PM, Hefter GT. Complexation of iron(III) and iron(II) by citrate. Implications for iron speciation in blood plasma. J. Inorg. Biochem. 2000; 78:175–184. [PubMed: 10805173]

39. Mills SA, Marletta MA. Metal binding characteristics and role of iron oxidation in the ferric uptake regulator from *Escherichia coli*. Biochemistry. 2005; 44:13553–13559. [PubMed: 16216078]

40. Mizuno K, Whittaker MM, Bächinger HP, Whittaker JW. Calorimetric studies on the tight binding metal interactions of *Escherichia coli* manganese superoxide dismutase. J. Biol. Chem. 2004; 279:27339–27344. [PubMed: 15082717]

41. Carver G, Tregenna-Piggott PLW, Barra A-L, Neels A, Stride JA. Spectroscopic and structural characterization of the $[Fe(imidazole)_6]^{2+}$ cation. Inorg. Chem. 2003; 42:5771–5777. [PubMed: 12950228]

42. Nistor A, Shova S, Cazacu M, Lazar A. Hexakis(1H-imidazole-κN^3)iron(II) sulfate–1H-imidazole (1/2). Acta Crystallogr. Sect. E Struct. Rep. Online. 2011; 67:m1600–m1601.

43. Singh PK, Parsek MR, Greenberg EP, Welsh MJ. A component of innate immunity prevents bacterial biofilm development. Nature. 2002; 417:552–555. [PubMed: 12037568]

44. Flo TH, et al. Lipocalin 2 mediates an innate immune response to bacterial infection by sequestrating iron. Nature. 2004; 432:917–921. [PubMed: 15531878]

45. Cartron ML, Maddocks S, Gillingham P, Craven CJ, Andrews SC. Feo – transport of ferrous iron into bacteria. BioMetals. 2006; 19:143–157. [PubMed: 16718600]

46. Stojilijkovic I, Cobeljic M, Hantke K. *Escherichia coli* K-12 ferrous iron uptake mutants are impaired in their ability to colonize the mouse intestine. FEMS Microbiol. Lett. 1993; 108:111–115. [PubMed: 8472918]

47. Konings AF, et al. *Pseudomonas aeruginosa* uses multiple pathways to acquire iron during chronic infection in cystic fibrosis lungs. Infect. Immun. 2013; 81:2697–2704. [PubMed: 23690396]

48. Velayudhan J, et al. Iron acquisition and virulence in *Helicobacter pylori*: a major role for FeoB, a high-affinity ferrous iron transporter. Mol. Microbiol. 2000; 37:274–286. [PubMed: 10931324]

Methods-only references

49. Carter P. Spectrophotometric determination of serum iron at the submicrogram level with a new reagent (ferrozine). Anal. Biochem. 1971; 40:450–458. [PubMed: 5551554]

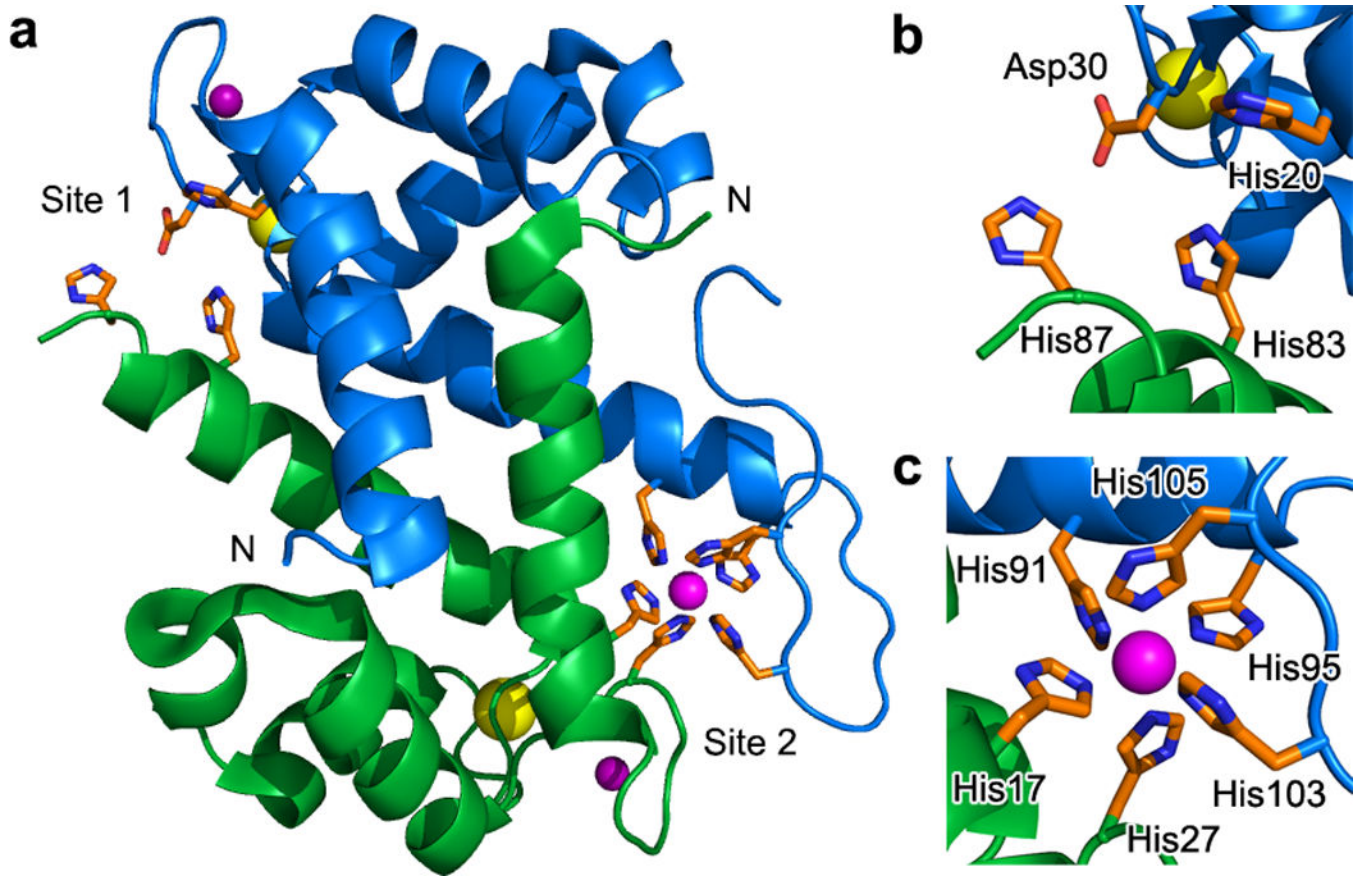

Figure 1. CP houses two transition-metal binding sites at the S100A8/S100A9 interface

(**a**) CP heterodimer from the structure of the Mn(II)-, Ca(II)-, and Na(I)-bound heterotetramer (PDB: 4XJK).[15] S100A8 is shown in green. S100A9 is shown in blue. The calcium ions are shown as yellow spheres. The sodium ions are shown as purple spheres. The manganese ion is shown as a magenta sphere. The amino acid residues at the metal binding sites are shown as orange sticks. (**b**) The His_3Asp motif (site 1) is comprised of (A8)His83, (A8)His87, (A9)His20, and (A9)Asp30. (**c**) The His_6 motif (site 2) is comprised of (A8)His17, (A8)His27, (A9)His91, (A9)His95, (A9)His103, and (A9)His105.

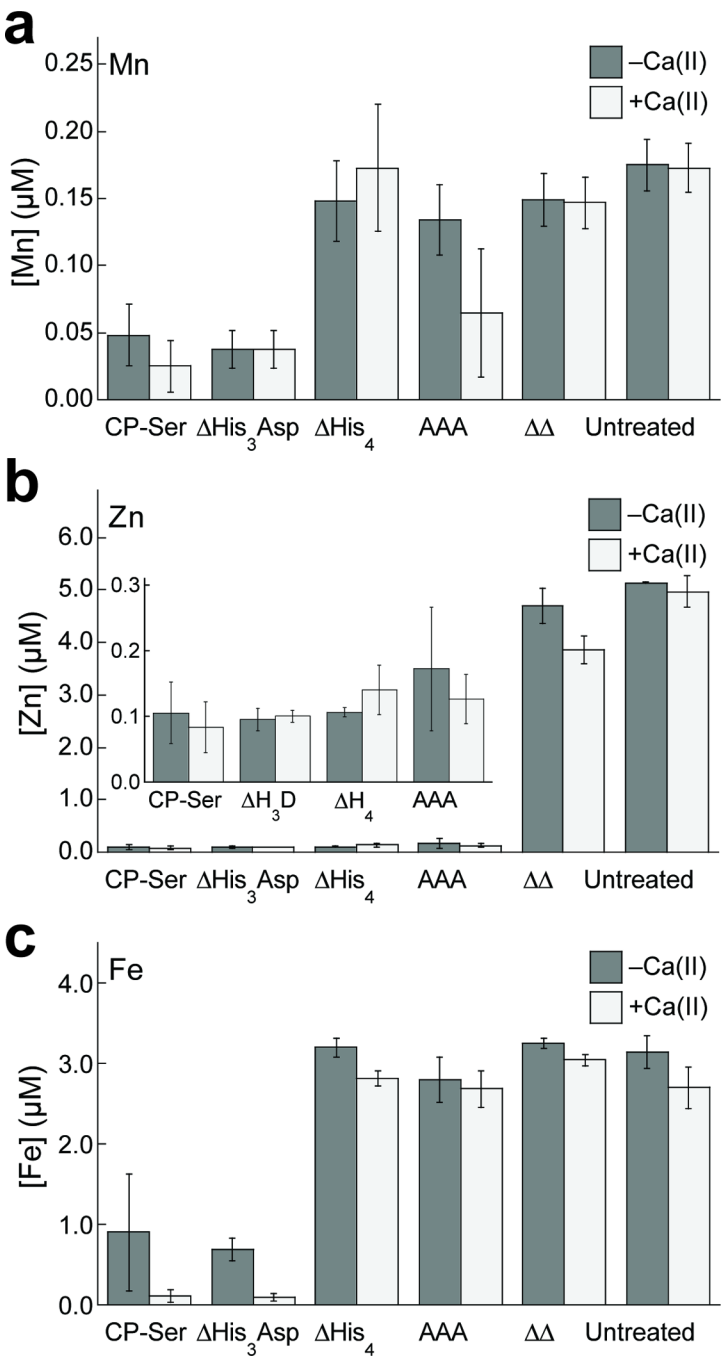

Figure 2. CP depleted metals from bacterial growth medium

Metal analysis of Mn (**a**), Zn (**b**), and Fe (**c**) concentrations in CP-treated and untreated growth medium (250 μg/mL CP, ~3 mM BME) in the absence (white bars) and presence (gray bars) of a 2-mM Ca(II) supplement (mean ± SEM, n ≥ 3).

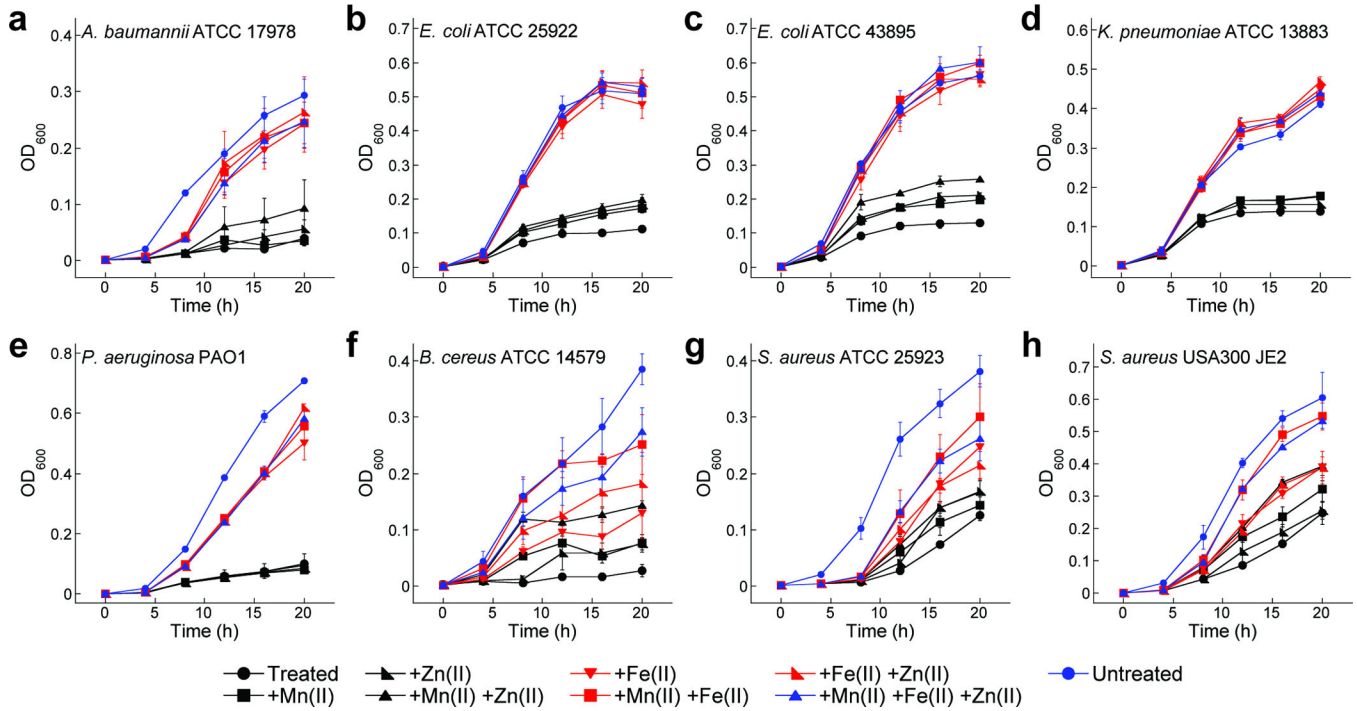

Figure 3. Metal supplementation growth studies

Growth curves of Gram-negative bacteria *Acinetobacter baumannii* (**a**), laboratory and enterohemorrhagic strains of *Escherichia coli* (**b,c**), *Klebsiella pneumoniae* (**d**), and *Pseudomonas aeruginosa* (**e**), and Gram-positive bacteria *Bacillus cereus* (**f**) and *Staphylococcus aureus* (**g,h**) cultured in medium (+Ca(II), +BME) treated with CP-Ser (250 μg/mL) and supplemented with 0.15 μM Mn(II), 3 μM Fe(II), and/or 5 μM Zn(II) (mean ± SEM, $n \geq 3$).

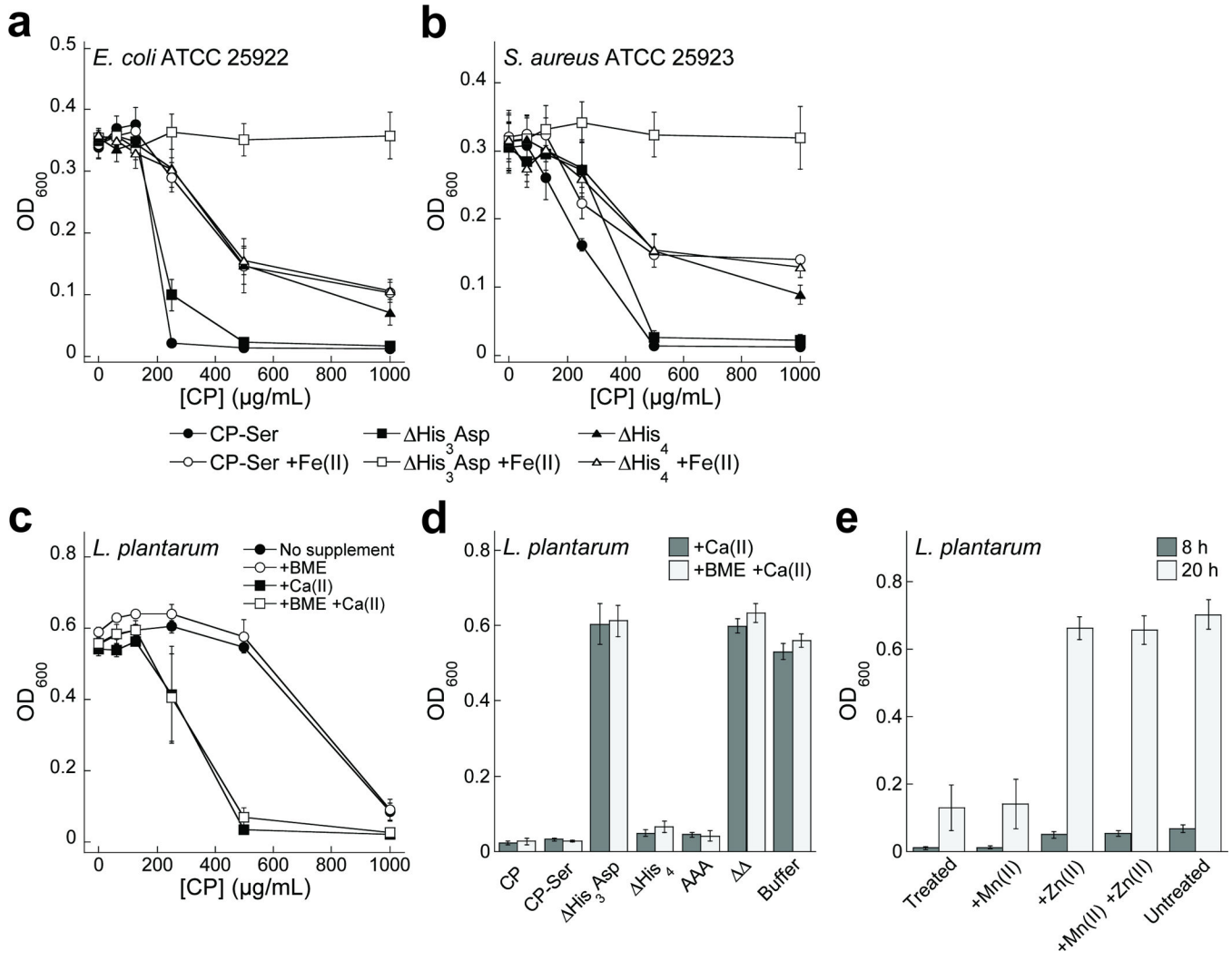

Figure 4. The antimicrobial activity of CP against *E. coli*, *S. aureus*, and *L. plantarum*

(**a,b**) Antibacterial activity of CP-Ser, ΔHis_3Asp, and ΔHis_4 preincubated with 0.9 equiv of Fe(II) against *E. coli* and *S. aureus* (t = 20 h, mean ± SEM, *n* = 6). (**c,d**) Antibacterial activity of CP against *L. plantarum* in the absence and presence of 2-mM Ca(II) and 3-mM BME supplements (t = 20 h, mean ± SEM, *n* = 3). (**e**) Growth of *L. plantarum* in medium treated with CP-Ser (500 μg/mL) supplemented with 10 μM Mn(II) and 10 μM Zn(II) (mean ± SEM, *n* = 3).

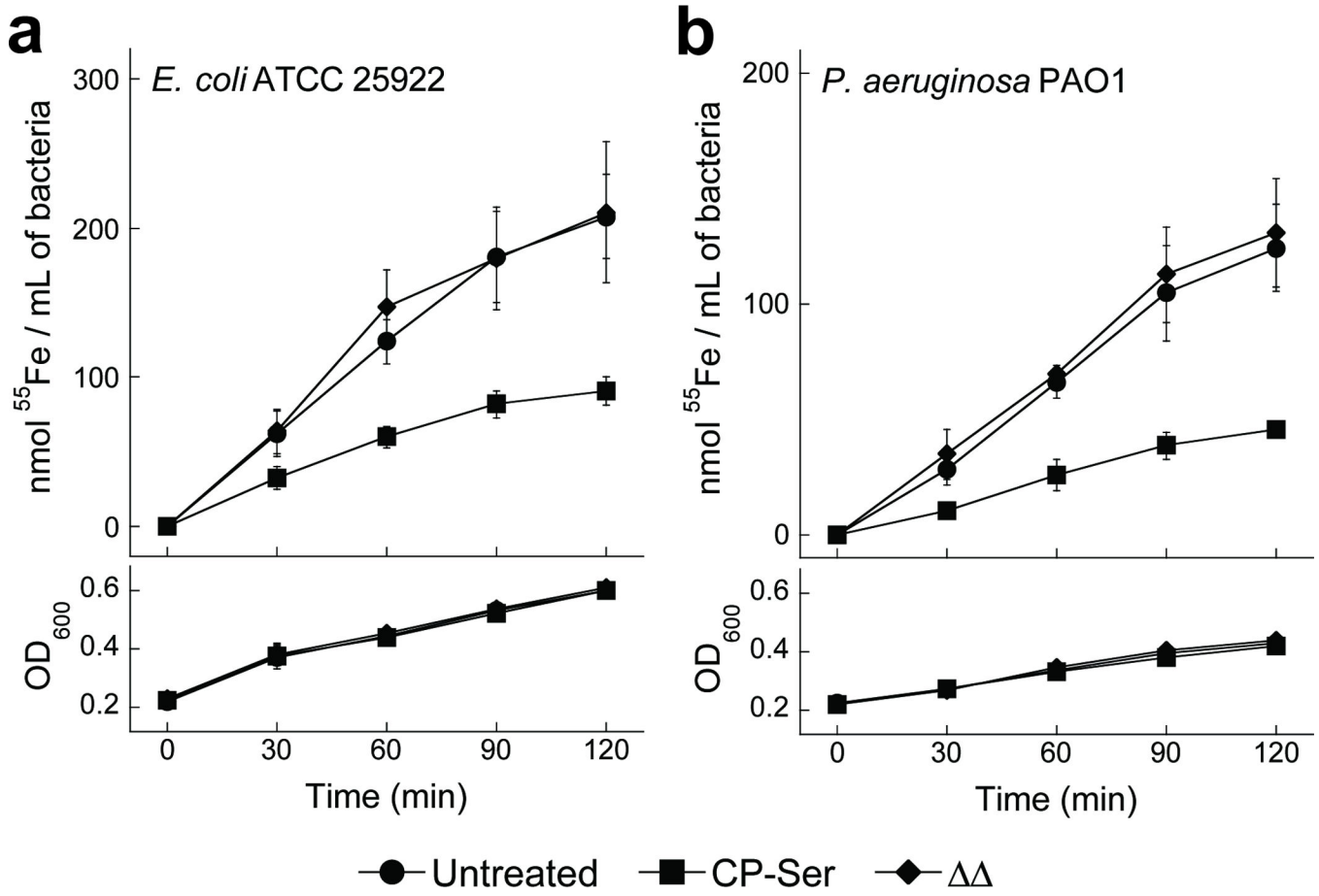

Figure 5. Inhibition of bacterial iron acquisition by CP

Uptake of radiolabeled ^{55}Fe by *E. coli* (**a**) and *P. aeruginosa* (**b**) treated with 500 μg/mL CP-Ser (squares) or ΔΔ (diamonds) compared with untreated bacteria (circles). The upper panels show the amount of ^{55}Fe uptake per mL of bacterial culture over the 2-h experiment. The lower panels indicate the corresponding OD_{600} values of the cultures at each time point. The mean ± SEM values for ^{55}Fe and OD_{600} are shown (n = 4).

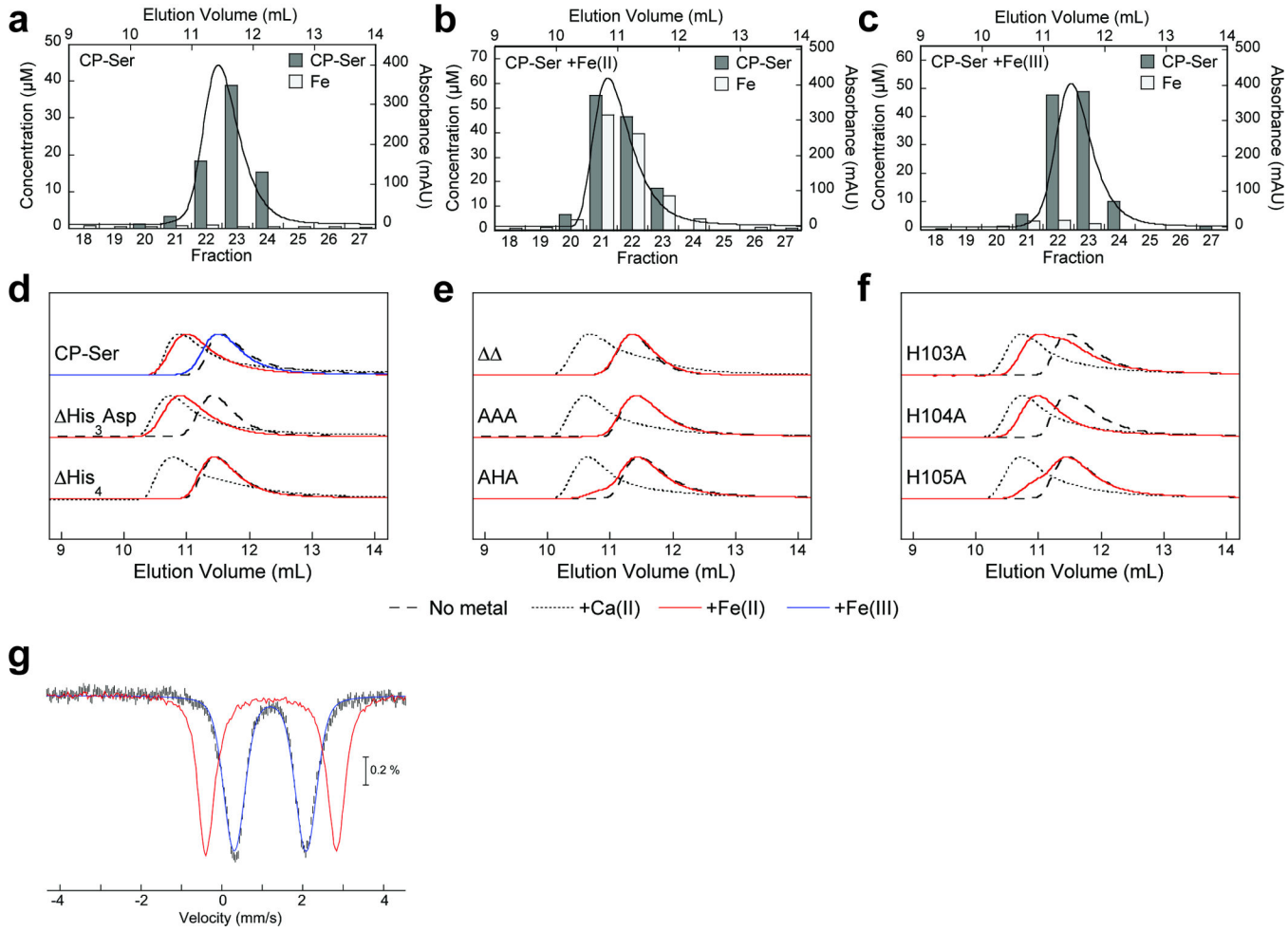

Figure 6. Hexahistidine Fe(II) coordination by CP

(**a–c**) Analytical SEC chromatograms of CP-Ser (400 μM) incubated with no metal, 5 equiv of Fe(II), and 5 equiv of Fe(III), and quantification of Fe and CP in eluent fractions. (**d–f**) Analytical SEC chromatograms of CP (20 μM) incubated with 10 equiv of Fe(II). Chromatograms for CP αβ (no metal) and $\alpha_2\beta_2$ (+Ca(II)) are provided for reference. Peak intensities are normalized to 1. (**g**) The 4.2-K/53-mT Mössbauer spectrum of ^{57}Fe(II)-bound CP-Ser (black vertical bars). Simulation using the parameters described in the main text is shown as the blue line, and the Mössbauer spectrum of Fe(II) sulfate in 50 mM Tris, pH 7.5 recorded under the same conditions is shown as the red line.

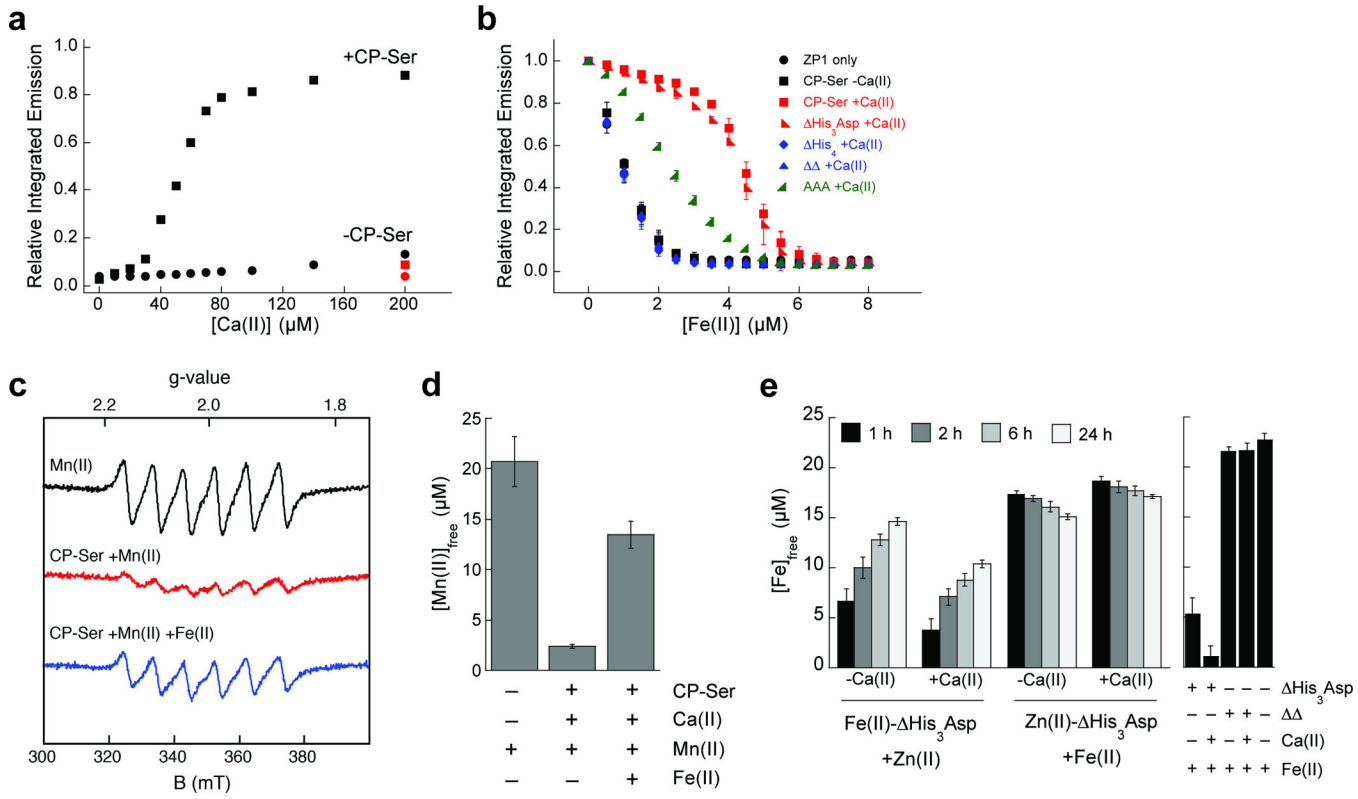

Figure 7. CP binds Fe(II) with remarkably high affinity in a Ca(II)-dependent manner

(**a**) ZP1 (1 μM) emission response to 3.5 μM Fe(II) in the absence (circles) and presence (squares) of 4 μM CP-Ser with addition of Ca(II). The red markers represent the 200-μM Ca(II) samples spiked with 4 μM Fe(II) (mean, *n* = 2). (**b**) ZP1 (1 μM) emission response to Fe(II) in the presence of 4 μM CP with or without 50 equiv of Ca(II) (mean ± SDM, *n* = 3). (**c**) Room-temperature EPR spectra of Mn(II) (black), CP-Ser in the presence of 50 equiv of Ca(II) and 0.9 equiv of Mn(II) (red), and CP-Ser in the presence of 50 equiv of Ca(II) and 0.9 equiv of Mn(II) with the addition of 0.9 equiv of Fe(II) (blue). (**d**) The concentration of free Mn(II) determined by room-temperature EPR (mean ± SDM, *n* = 3). (**e**) The concentration of unbound Fe(II) in ΔHis_3Asp samples containing 0.9 equiv of Fe(II) after addition of 0.9 equiv of Zn(II) with and without 50 equiv of Ca(II) (mean ± SDM, *n* = 3). Control samples containing 25 μM protein, 0.9 equiv of Fe(II), and/or 50 equiv of Ca(II) are described in the right panel.